

PATH PLANNING FOR AUTOMOTIVE COLLISION AVOIDANCE BASED ON ELASTIC BANDS

Thorsten Brandt, Thomas Sattel

*L-LAB: Public Private Partnership of
University of Paderborn and Hella KGaA Hueck & Co.
Heinz Nixdorf Institute, Mechatronics and Dynamics,
Fuerstenallee 11, D-33102 Paderborn, Germany;
{tb, sattel}@hni.upb.de*

Abstract: Collision-free path planning will be an essential feature of future automotive collision avoidance systems (CAS). One of the most promising approaches uses so-called elastic bands in generating emergency trajectories. For the automotive application of this approach, moving obstacles and the borders of the road are modeled by virtual potential fields. To find solutions even in complex driving situations, the concept of computing several possible trajectories instead of just one is introduced. The stability of a vehicle traveling along these trajectories is estimated based on a model. A suitable estimation method and sample simulation results are given. *Copyright © 2005 IFAC*

Keywords: obstacle avoidance, path planning, automotive control, autonomous vehicles, vehicle dynamics.

1. INTRODUCTION

Recent developments in automotive sensor technology have promoted the improvement of existing safety and assistance systems and allow the exploration of new areas of application. All indications are that, within the coming years, further improvements in the environmental data collected by sensor fusion of systems such as radar, lidar, laser scanners, and video systems can be expected (Vukotich and Kirchner, 2001). Given sufficiently high quality data about positions and velocities of static objects and moving traffic participants, future vehicles might be able to navigate autonomously through the traffic. In these autonomous vehicles, emergency features such as collision avoidance will be essential. For the time being, as an intermediate step, it seems reasonable to consider collision avoidance systems (CAS) that take over the driving task in emergency situations that a human driver cannot handle.

A key feature of CAS will be the generation of emergency trajectories. In this paper, a promising

path-planning technique is presented. The method of elastic bands is adapted from robotics and modified in a way that allows appropriate solutions for automotive applications to be found. In this method, an elastic band consists of nodes connected by springs. One end of the elastic band is fixed to the vehicle, as depicted in Fig. 1. Moving obstacles and the borders of the road are modeled by repulsive virtual potential fields, which deform the band.

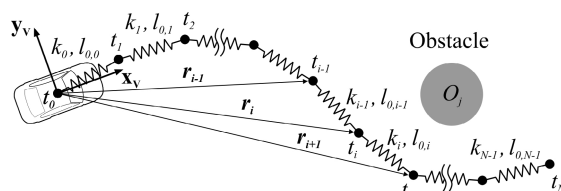


Fig. 1: Single elastic band described in a vehicle fixed reference frame (x_v, y_v) and an obstacle O_j

Several emergency trajectories, instead of just one, are computed in order to find possible collision-free paths even in complex driving situations. The equilibrium positions of the nodes of the elastic bands are determined numerically using a suitable

algorithm outlined in this paper. Subsequently, the smooth transition between the nodes in the equilibrium configurations is carried out by a spline interpolation. The final path is then selected by a given criterion.

Although emergency trajectories can be generated, it cannot generally be guaranteed that a vehicle moves stably on a planned trajectory. Thus, it is necessary to predict the driving conditions based on a model. An adequate model and an applicable evaluation method for the stability of the lateral motion of the vehicle are mentioned.

A possible overall structure of a CAS composed of the previously described components is presented. Finally, sample simulation results for an emergency maneuver are given.

2. ELASTIC BANDS

The concept of elastic bands was introduced by Quinlan and Khatib (Quinlan and Khatib, 1993) for robotic path planning. Subsequently, Hilgert et al. (Hilgert, *et al.*, 2001) and Gehring and Stein (Gehring and Stein, 2001) applied the concept to automotive problems. Their main focus lay on vehicle following and lane change maneuvers. Because path planning with elastic bands is local, the method may fail to find existing collision-free solutions when the changes in the environment are large (Quinlan and Khatib, 1993). However, in traffic situations, the environmental changes cannot generally assumed to be small. Examples of sudden changes can be a truck that loses its payload on the initially planned path or a vehicle that could not be detected by the sensors because it was hidden behind another vehicle. Therefore, the method of elastic bands needs to be modified for automotive collision avoidance systems.

2.1 Generation of Several Elastic Bands starting from an initially planned path

In this approach, obstacles are modeled by safety circles, which should not be penetrated by the path of the center of gravity of the CAS-equipped vehicle, as depicted in Fig. 2. The diameter d_j of the safety circle of obstacle O_j consists of the sum of the diameter of the circle that completely covers the obstacle and the width of the CAS-equipped car.

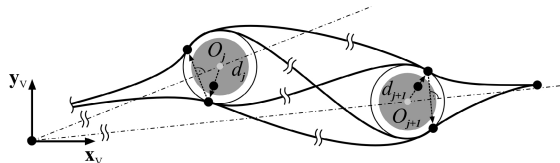


Fig. 2: Several elastic bands avoiding two obstacles O_j and O_{j+1}

As soon as the estimated collision risk exceeds a particular threshold value, the planning of an

emergency path starts; this point in time is denoted t_0 . The generation of a drivable trajectory must be finished within a given time limit T_{max} , otherwise emergency braking without steering should be initiated. All nodes of the initially planned path that lie within the safety circle of an obstacle O_j are shifted along the shortest vector into a small neighborhood outside of the safety circle, as shown in Fig. 2. In general, it cannot be anticipated whether passing an obstacle on the left or on the right is preferable.

Therefore, all shifted nodes are reflected across the line pointing from the origin of the vehicle fixed reference frame (x_v, y_v) to the center of the corresponding safety circle. For k obstacles through which the original trajectory passes, this permutation yields 2^k elastic bands as illustrated in Fig. 2. These elastic bands are influenced by the repulsive potential fields of the obstacles and the borders of the road. Emergency trajectories are generated by determination of the equilibrium positions of these bands. After interpolation with time-parameterized splines, the emergency trajectory with the smallest maximum lateral acceleration is selected. In doing so, the lateral acceleration is estimated by

$$a_n(t) = v_x(t)^2 \kappa(t) \quad , \quad (1)$$

where $v_x(t)$ and $\kappa(t)$ denote the planned longitudinal velocity of the CAS-equipped vehicle and the curvature of the emergency trajectory at time t , respectively. The curvature is calculated by

$$\kappa(t) = \frac{\dot{x}_v \ddot{y}_v - \dot{y}_v \ddot{x}_v}{(\sqrt{\dot{x}_v^2 + \dot{y}_v^2})^3} \quad , \quad (2)$$

where $(x_v(t), y_v(t))$ denote the time-parameterized emergency paths. Once a trajectory has been selected with (1) at time $t_0 + \Delta T$ ($\Delta T < T_{max}$), that trajectory, virtually lying on the road surface, is now detached from the CAS-equipped vehicle and driven along by the vehicle at the planned longitudinal velocity $v_x(t)$.

2.2 Internal Potentials of an Elastic Band

The nodes of an elastic band are described in the vehicle fixed reference frame (x_v, y_v) by two-dimensional vectors \mathbf{r}_i , as depicted in Fig. 1. Therein, the nodes are numbered in temporally ascending order with $i=0, \dots, N$: $t_i > t_{i-1}$. The internal potential of each interval is modeled by the potential of a linear spring

$$V_i^{\text{int}} = \frac{1}{2} k_i (\|\mathbf{r}_{i+1} - \mathbf{r}_i\| - l_{0,i})^2 \quad , \quad (3)$$

where $l_{0,i}$ and k_i denote the initial spring length and the spring stiffness in interval i , respectively. The used Euclidean norm is defined as

$$\|\mathbf{r}_{i+1} - \mathbf{r}_i\| = \sqrt{(r_{i+1,x} - r_{i,x})^2 + (r_{i+1,y} - r_{i,y})^2} \quad (4)$$

The internal potential of the entire elastic band can be expressed as

$$V^{\text{int}} = \sum_{i=0}^{N-1} V_i^{\text{int}} = \frac{1}{2} \sum_{i=0}^{N-1} k_i (\|\mathbf{r}_{i+1} - \mathbf{r}_i\| - l_{0,i})^2 \quad (5)$$

2.3 External Potentials of the Borders of the Road

The virtual potential field of the borders of the road is defined in a way that its absolute value decreases logarithmically towards the middle of the road. The borders are assumed to be continuous. To evaluate the potential of the borders at the nodes of the elastic bands, reference points at the borders having normal vectors pointing toward the corresponding nodes are chosen. The potential is defined separately for the left and the right border

$$V^{B_q}(\mathbf{r}_i) = k^{B_q} \ln \|\mathbf{r}_i - \mathbf{r}_i^{B_q}\| \quad \text{with } q \in \{l, r\}, \quad (6)$$

with k^{B_q} being the constants of the nonlinear springs as shown in Fig. 3. The vector $\mathbf{r}_i^{B_q}$ denotes the position vector of the reference point at the border for node i of the elastic band in the vehicle fixed reference frame.

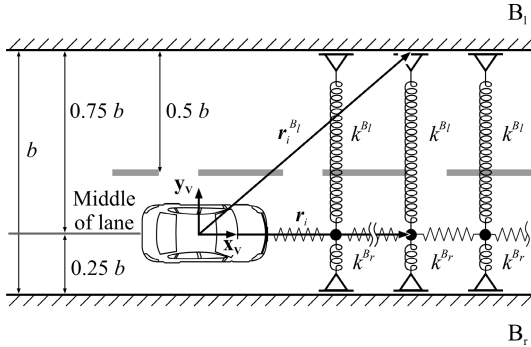


Fig. 3: Neutral position of an elastic band

The forces acting from the borders on the nodes of the bands are calculated by taking the directional derivatives with respect to the position vector \mathbf{r}_i

$$\mathbf{F}_i^{B_q} = \frac{\partial V_i^{B_q}}{\partial \mathbf{r}_i} := \frac{k^{B_q}}{\|\mathbf{r}_i - \mathbf{r}_i^{B_q}\|} \cdot \frac{\mathbf{r}_i - \mathbf{r}_i^{B_q}}{\|\mathbf{r}_i - \mathbf{r}_i^{B_q}\|} \quad (7)$$

For parallel borders, in absence of obstacles, the equilibrium position of the elastic band can for example be adjusted at the middle of the right lane. In doing so, force equilibrium $\mathbf{F}_i^{B_l} = \mathbf{F}_i^{B_r}$ yields

$$\frac{k^{B_l}}{k^{B_r}} = \frac{0.75b}{0.25b} = 3 \quad (8)$$

Alternatively, the potentials of the borders can be chosen in a way that the corresponding forces are limited, even for small distances to the border

$$\mathbf{F}_i^{B,q} = k^{B,q} e^{-\|\mathbf{r}_i - \mathbf{r}_i^{B_q}\|} \cdot \frac{\mathbf{r}_i - \mathbf{r}_i^{B_q}}{\|\mathbf{r}_i - \mathbf{r}_i^{B_q}\|} \quad (9)$$

2.4 External Potentials of Moving Obstacles

Similar to the borders of the road, the obstacles are modeled by repulsive continuously differentiable potential fields. Compared to potentials that are only locally effective and not continuous, it turned out that globally effective potential fields have numerical advantages in finding the equilibrium configurations. Analogous to the potentials of the borders of the road, potentials of obstacles are modeled as functions that logarithmically decay with the distance to the obstacles. The potential field of obstacle O_j , evaluated at node i of an elastic band becomes

$$V^{O_j}(\mathbf{r}_i) = k^{O_j} \ln \left(\|\mathbf{r}_i - \mathbf{r}^{O_j}\| - \frac{d_j}{2} \right) \quad (10)$$

However, as indicated in Fig. 4, each node i of the elastic band is driven through by the vehicle at a different instant of time t_i , according to the planned longitudinal velocity $v_x(t)$.

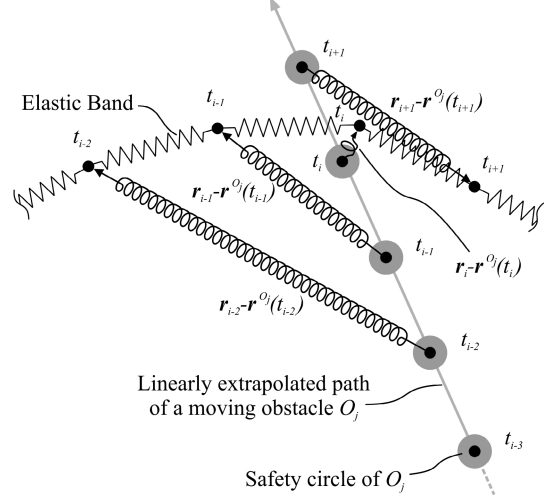


Fig. 4: Incorporation of a moving obstacle O_j

The motion of the obstacles is linearly extrapolated for the moments t_0 to t_N based on sensor data measured at time t_0 . As a consequence, the velocity vector of an obstacle is assumed to be constant. Because of the motion of the obstacles, the potential of an obstacle O_j evaluated at node i of an elastic band has to be evaluated with the corresponding position of O_j at time t_i

$$V^{O_j}(\mathbf{r}_i) = k^{O_j} \ln \left(\|\mathbf{r}_i - \mathbf{r}^{O_j}(t_i)\| - \frac{d_j}{2} \right) \quad (11)$$

The repelling forces acting on the nodes of an elastic band are calculated by the directional derivatives of the potentials with respect to the position vector \mathbf{r}_i

$$\mathbf{F}_i^{O_j} = \frac{\partial V^{O_j}(\mathbf{r}_i)}{\partial \mathbf{r}_i} := \frac{k^{O_j}}{\|\mathbf{r}_i - \mathbf{r}^{O_j}(t_i)\| - \frac{d_j}{2}} \cdot \frac{\mathbf{r}_i - \mathbf{r}^{O_j}(t_i)}{\|\mathbf{r}_i - \mathbf{r}^{O_j}(t_i)\|} \quad (12)$$

Alternatively, a formulation analogous to (9) for the forces of the obstacles is also useful

$$\mathbf{F}_i^{O_j} = k^{O_j} e^{-\left(\frac{\|\mathbf{r}_i - \mathbf{r}_i^{B_{O_j}}\|}{2}\right)^2} \cdot \frac{\mathbf{r}_i - \mathbf{r}_i^{B_{O_j}}}{\|\mathbf{r}_i - \mathbf{r}_i^{B_{O_j}}\|} \quad (13)$$

2.5 Determination of Equilibrium Solutions

The forces at each node are given by the directional derivatives of the corresponding potential fields. At each node, force equilibrium leads to

$$\mathbf{F}_i^{sum} = \mathbf{F}_i^{int} + \mathbf{F}_i^{B_1} + \mathbf{F}_i^{B_2} + \sum_{j=1}^M \mathbf{F}_i^{O_j} = 0 \quad (14)$$

Therein, the forces of the borders of the road and the obstacles are nonlinear. Thus, (14) can only be solved numerically for the position vectors of the nodes of the elastic bands. A Newton-Raphson method is employed for this task. In this method the Jacobian of the forces acting on each node is needed. The Jacobian of the forces is given by

$$\mathbf{J} = \frac{\partial \mathbf{F}_i^{sum}}{\partial \mathbf{r}_i} \quad (15)$$

Because the external forces depend only on the position vector of the node at which they are evaluated, nonzero derivatives of the external forces occur only on the main diagonal of (15). However, in addition to the position vector of the node, the internal forces also depend on the position vector of the preceding and the following node. Thus, \mathbf{J} has tridiagonal form. Node 0 is fixed at the CAS-equipped vehicle and node N can arbitrarily be placed on the road. Combining the position vectors of nodes 1 to $N-1$ in one array $\mathbf{q} = [\mathbf{r}_1, \dots, \mathbf{r}_i, \dots, \mathbf{r}_{N-1}]^T$ and the corresponding forces into one array \mathbf{F} , the following system can be set up

$$\mathbf{J}(\mathbf{q}^{old}) \Delta \mathbf{q} = -\mathbf{F}(\mathbf{q}^{old}), \quad \mathbf{q}^{new} = \mathbf{q}^{old} + \Delta \mathbf{q} \quad (16)$$

and iteratively solved for $\Delta \mathbf{q}$ until all components of $\Delta \mathbf{q}$ are smaller than a value ϵ . In the iterations, it must be enforced that no node leaves the borders of the road or penetrates the safety circle of an obstacle. If a $\Delta \mathbf{q}$ shifts a node into such a non-valid area, the node is still moved along the same displacement vector, but by a smaller distance. If the distance from a node $i+1$ to node 0 is smaller than the distance from node i to node 0, which means that the band starts twisting, the spring stiffness k_i of interval i gets increased. Alternatively, the stiffness of all intervals can be increased. After each iteration, it has to be determined at which time each node is driven through by the vehicle in order to evaluate the positions of the obstacles at the same times. An

approximate evaluation can be performed by use of straight lines through all nodes.

3. VEHICLE MODEL

A widely used model in lateral vehicle dynamics is the bicycle model as shown in Fig. 5. The main idea of this planar model is to combine the two tires of each axle into a single tire.

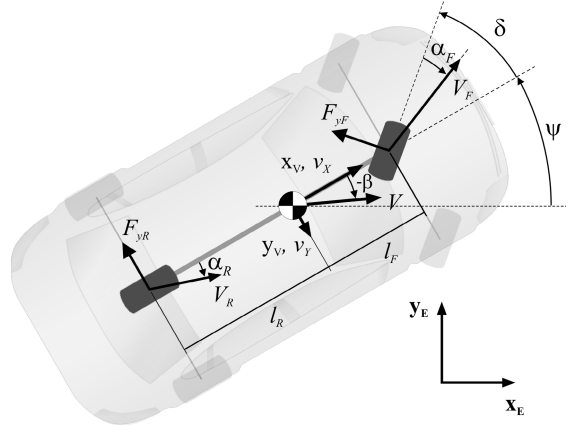


Fig. 5: Bicycle model with vehicle and earth fixed reference frame (x_V, y_V) and (x_E, y_E) , respectively

Up to lateral accelerations of $0.4g$, with g being the gravitational constant, linearization of the model about a fixed velocity V provides reliable results. More than 80% of typical driving situations can be covered by this. However, for emergency maneuvers it cannot be guaranteed that only low lateral accelerations occur. Therefore, a nonlinear bicycle model is strongly recommended for CAS. One of the main problems in linearizing the bicycle model is that the lateral forces at the tires are linearized and therefore are not limited. The equations of motion for a nonlinear bicycle model, including a simple model for the power train, can be found in (Smith and Starkey, 1995).

Nevertheless, in the subsequent simulations, a linear bicycle model is employed for two reasons: avoiding the control of the longitudinal motion and highlighting the fact that a linear model can suggest stable motion even if the maximum tire forces have already been exceeded. The equations of motion of the employed model are (Isermann, 2001)

$$\begin{bmatrix} \dot{\beta} \\ \ddot{\psi} \end{bmatrix} = \mathbf{A} \begin{bmatrix} \beta \\ \dot{\psi} \end{bmatrix} + \mathbf{B} \delta \quad (17)$$

with

$$\mathbf{A} = \begin{bmatrix} -\left(\frac{c_{\alpha F} + c_{\alpha R}}{Vm}\right) & \left(\frac{-c_{\alpha F} l_F + c_{\alpha R} l_R}{V^2 m} - 1\right) \\ \left(\frac{-c_{\alpha F} l_F + c_{\alpha R} l_R}{J_z}\right) & -\left(\frac{c_{\alpha F} l_F^2 + c_{\alpha R} l_R^2}{V J_z}\right) \end{bmatrix} \quad (18)$$

and

$$\mathbf{B} = \begin{bmatrix} \frac{c_{\alpha F}}{Vm} & \frac{c_{\alpha F} l_F}{J_z} \end{bmatrix}^T \quad (19)$$

The states of the model are the side slip angle β and the yaw rate $\dot{\psi}$ as depicted in Fig. 5. The only control input is given by the steering angle δ . The parameters of the simulation model are summarized in Tab. 1.

Table 1: Vehicle parameters

Symbol	Description	Value	Unit
m	Vehicle mass	1280	[kg]
J_z	Moment of inertia about z_V -axis	2500	[kgm ²]
l_F	Distance of front axle to C.G.	1.203	[m]
l_R	Distance of rear axle to C.G.	1.217	[m]
c_{aF}	Front tire cornering stiffness	100000	[N/rad]
c_{aR}	Rear tire cornering stiffness	100000	[N/rad]

4. STABILITY ESTIMATION

The stability of the lateral motion is estimated by the so-called Characteristic Velocity Stability Indicator CVSI (Börner, *et al.*, 2002). The CVSI is determined by comparisons of the longitudinal velocity of the vehicle, $v_x(t)$, and its characteristic velocity

$$v_{ch}^2(t) := \frac{v_x^2(t)}{1 - \frac{\delta(t) v_x(t)}{\dot{\psi}(t) i_{st} l}} \quad (20)$$

The corresponding driving conditions to the CVSI values are given in Tab. 2.

Table 2: Interpretation of CVSI values

CVSI	Driving condition
1	Under-steering, stable
2	Neutral-steering, stable
3	Over-steering, stable
4	High-over-steering, indifferent
5	Braking away, unstable

5. CAS: OVERALL SYSTEM SETUP

A possible overall system setup of a CAS is illustrated in Fig. 6. The path planning algorithm provides possible emergency trajectories based on the available sensor data. The path following controller computes corresponding steering angle, acceleration and braking signals, which allow the vehicle to follow the planned trajectories. Before these signals are sent to the actuators of the vehicle, the stability of the vehicle for the proposed signals is estimated based on a model, employing the CVSI as shown in Fig. 6. If the CVSI indicates that the vehicle would brake away on the proposed trajectory, an alternative needs to be planned. For drivable

emergency trajectories, the corresponding control signals are sent to actuators. Sensors permanently observe the state of the vehicle and the environment. If an obstacle moves differently as assumed for the path planning, this can be incorporated in the next time step.

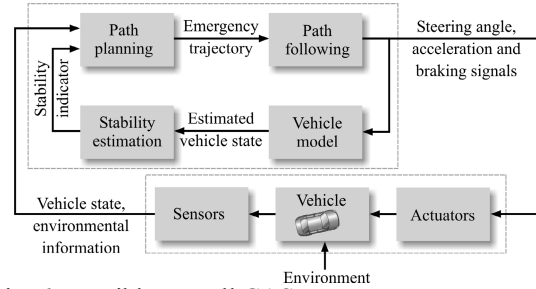


Fig. 6: Possible overall CAS setup

6. SIMULATION RESULTS

In order to demonstrate how the path planning procedure can be embedded in the overall setup, path following is performed by a simple PID-controller which minimizes the lateral displacement between the planned and actually driven path. With such a PID-controller it is possible to follow emergency trajectories for various evasion scenarios. However, the deficiency of such a simple controller is illustrated in the following. Examples of more sophisticated path following strategies can for example be found in (Freund and Mayr, 1997).

In the simulated scenario a CAS-equipped car drives at a speed of 20 m/s on a 7 m wide road. At time t_0 a non-moving obstacle, for example lost payload of a truck, appears 40 m ahead. In the other lane, an oncoming vehicle travels at 15 m/s from an initial distance of about 120 m. The simulation parameters for the path planning are summarized in Tab. 3.

Table 3: Path planning parameters

Symbol	Description	Value	Unit
d_1	Safety diameter of oncoming vehicle	4	[m]
d_2	Safety diameter of non-moving obstacle	2.5	[m]
k^{O_1}	Force scaling factor of oncoming vehicle	1	[-]
k^{O_2}	Force scaling factor of non-moving obstacle	1	[-]
k^{B_l}	Force scaling factor of left border	8	[-]
k^{B_r}	Force scaling factor of right border	$8e^{-24.5}$	[-]
k_i	Initial internal spring stiffness for all intervals	1	[N/m]
$l_{0,i}$	Initial length of internal springs	1	[m]
N	Number of nodes	41	[-]

The forces of the borders of the road and the obstacles were modeled according to (9) and (13),

respectively. In Fig. 7 the results for the steering angle, the yaw rate, the lateral acceleration and the CVSI of the CAS-equipped vehicle are graphed. In the simulation the vehicle followed the planned path with a maximum error smaller than 0.2 m. However, it can be seen that the CVSI indicates several critical driving conditions. The reason is, that the parameters of the PID-controller are constant for all possible paths to follow. Since the control variables are not limited, the tire forces can be exceeded. This leads to critical driving conditions for some paths as in the given example. Therefore, a more sophisticated path following controller should take nonlinear effects as saturation of the tire forces into account.

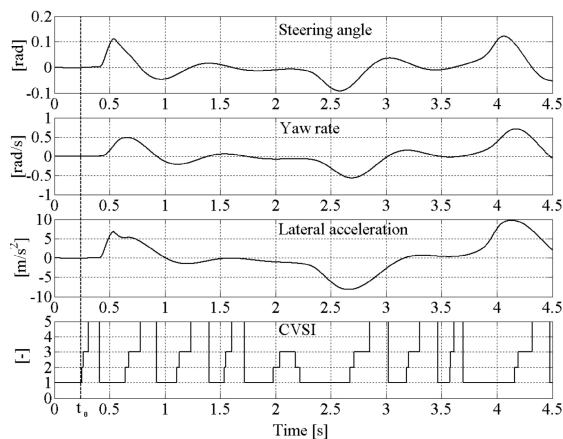


Fig. 7: Simulation results of the CAS-equipped vehicle following the emergency trajectory based on a linear bicycle model

The simulated evasion maneuver is illustrated in Fig. 8. The CAS-equipped vehicle and the oncoming vehicle are displayed at corresponding times. Therein, the oncoming vehicle and the non-moving obstacle are represented by their safety circle.

7. CONCLUSIONS

The method of elastic bands was modified in a way to create collision-free trajectories even in complex traffic situations. Accordingly, it was presented how several elastic bands can be generated intermediately and a single solution can be selected afterwards. Also the modeling of the borders of the road and moving obstacles by virtual nonlinear fields was illustrated. The stability of a CAS-equipped vehicle traveling on an emergency trajectory generated by use of elastic bands was estimated with the Characteristic Velocity Stability Indicator (CVSI) based on a bicycle model. A possible overall control structure of CAS was outlined and simulation results for a sample emergency maneuver were given. In this simulation the fact was stressed, that nonlinear path following control should be addressed in future work.

ACKNOWLEDGEMENTS

Many thanks to the *L-LAB* and the *International Graduate School of Dynamic Intelligent Systems* in

Paderborn for supporting this work with facilities and a research scholarship.

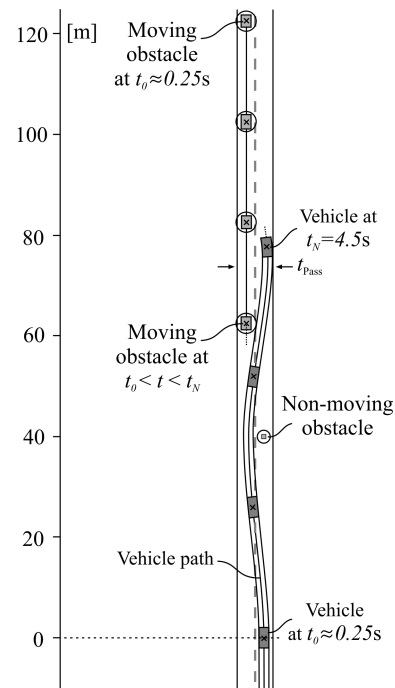


Fig. 8: Evasion maneuver

REFERENCES

- Börner, M., Andréani, L., Albertos, P. and Isermann, R. (2002). *Detection of Lateral Vehicle Driving Conditions Based on the Characteristic Velocity*. IFAC World Congress 2002, 21.-26. July, Barcelona, Spain.
- Freund, E., Mayr, R. (1997). *Nonlinear Path Control in Automated Vehicle Guidance*, IEEE Trans. Robot. Autom., Vol. 13, No. 1, February 1997
- Gehring, S.K. and Stein, F.J. (2001). *Elastic Bands to Enhance Vehicle Following*. IEEE Intelligent Transportation Systems Conf. Proc., Oakland (CA), USA
- Hilgert, J., Hirsch, K., Bertram, T. and Hiller, M. (2003). *Emergency Path Planning for Autonomous Vehicles Using Elastic Band Theory*. IEEE/ASME Int. Conf. on Advanced Intelligent Mechatronics AIM 2003, July 20-24, Kobe, Japan.
- Isermann, R. (2001). *Diagnosis Methods for Electronic Controlled Vehicles*. Vehicle Systems Dynamics, Vol. 36, No. 2-3, pp. 77-117
- Smith D.E. and Starkey, J.M. (1995). *Effects of Model Complexity on the Performance of Automated Vehicle Steering Controllers: Model Development, Validation and Comparison*. Vehicle Systems Dynamics, 24, pp. 163-181
- Quinlan, S. and Khatib, O. (1993). *Elastic Bands: Connecting Path Planning and Control*. IEEE Int. Conf. on Robot. and Autom., vol. 2, pp. 802-807, Atlanta (GA), USA
- Vukotich, A. and Kirchner, A. (2001). *Sensorfusion für Fahrerassistenzsysteme*. VDI Berichte 1646, pp. 857, VDI-Verlag, Düsseldorf, Germany.